Journal of Applied Engineering Science & Technology Vol. 6 No. 3 (2026) 168 Special Issue: CMEME 2025

Issues lists available at UMKB journals

Journal of Applied Engineering Science & Technology

Journal home page: https://journals.univ-biskra.dz/index.php/jaest

https://doi.org/10.69717/jaest.v6.i3.168 Research Article

Effect of calcination treatment on the in vitro bioactivity of ceramic powders

Djahida Sidane[1,*], Nadir Slimani[1], Yasmina Bourebaba[2], Nawal Deflaoui[1], Lynda Sadou[1], Hafit Khireddine[1]

[1]*Université de Bejaia, Faculté de Technologie, Laboratoire de Génie de l'Environnement (LGE), 06000 Bejaia, Algeria*
[2]*Université de Bejaia, Faculté des Sciences de la Nature et de la Vie, Laboratoire de Biomathématique, Biophysique, Biochimie et Scientométrie (L3BS), 06000 Bejaia, Algeria*

ABSTRACT

The aim of this study was to evaluate the effect of varying calcination temperature and duration (500°C -1h, 600°C-1h, 600°C-6h, and 900°C-3h) on the bioactivity property of crystalline hydroxyapatite pellets immersed in a physiological solution (simulated body fluid) for 7 days. The microstructural properties and composition of the powders–such as the degree of crystallinity, crystallite size, additional thermal phases of β-tricalcium phosphate (β-TCP) and CaO, and functional groups (hydroxyl and carbonate)–vary depending on the calcination parameter and immersion process. X-ray diffraction (XRD) and infrared spectroscopy (IR) analyses showed significant microstructural changes for the HAP calcined at 900°C for 3 hours. Moreover, atomic absorption spectroscopy (AAS) analysis and pH measurements indicated variations in calcium ion concentration (42.2 ± 0.70 mg/L after 3 days, and 34.2 ± 0.48 mg/L after 7 days of immersion time) and pH of the medium-which decreased from 7.440 ± 0.02 to 7.305 ± 0.03-for the HAP pellet calcined at 900°C. These results were confirmed by X-ray fluorescence (XRF) and electron microscopy, which indicated an increase in the Ca content from 55.06 ± 0.156% to 55.85±0.148%, and in the P content from 24.64±0.155% to 27.59±0.158%, as well as the deposition of dispersed particles and large agglomerates, suggesting the formation of a non-uniform layer of calcium phosphate (CaP) on the surface of the powder pellet calcined at 900°C.

KEYWORDS

Calcium phosphate
Calcination
Bioactivity
Physiological solution
Bioceramic powder
Tissue engineering

ARTICLE HISTORY	Received	Revised	Accepted	Published
	07 Apr 2026	03 Aug 2026	21 Aug 2026	19 Sept 2026

1 Introduction

Ceramic biomaterials, particularly calcium phosphate bioceramic, are widely used for bone replacement applications due to their good biological and physicochemical properties [1]. In order to expand their areas of application, their biological and mechanical performance must be improved to promote, for example, cell adhesion and proliferation or implantation in sites subject to heavy loads, through the use of biocomposite material systems [2-5]. Among the fundamental characteristics that must be verified on active ceramic biomaterials is the ability to form a "Bone-like apatite" layer on their surface. In this context, numerous studies have reported the effect of combining ceramic powders with other functional materials in order to improve their bioactivity property through the formation of a surface layer of hydroxycarbonate apatite in contact with bone tissue [6-9]. However, few studies have been published on the effect of calcination treatment on the bioactive properties of calcium phosphate powders. One example is the work by Forero-Sossa et al. [10], who studied the effect of calcination temperature on the physicochemical and bioactive properties of biogenic hydroxyapatite; they concluded that samples calcined at high temperatures (around 1000°C and between 1100 and 1200°C) exhibited changes associated with the formation of bone-type apatite on the surface of the samples, and observed that the presence of a tricalcium phosphate phase resulted in a higher reaction rate.

In this study, the effect of calcination treatment on the bioactivity of calcium phosphate powders synthesized by the sol-gel process was investigated in vitro in the presence of a physiological solution (SBF) simulating the biological environment of the human body, as reported by Kokubo and Takadama [11]. The synthesized powders can be considered bioactive if they induce the formation of an apatite layer on their surface via chemical bonds in the SBF medium [12]. The interaction between the ions contained in the SBF solution (mainly Ca^{2+} and PO_4^{3-}) and the material in contact was evaluated by analyzing the microstructure and composition of the materials as well as the physiological media collected after immersing the material for 7 days. It is known that most of bioactive ceramics in clinical use show apatite-forming ability in the physiological solution within 7 days [13]. Moreover, the SBF immersion test, used to evaluate the bioactivity of CaP materials in contact with bone, revealed the deposition of an apatite layer on their surface within 7 days [14]. Accordingly, in order to evaluate the effect of varying calcination

* Corresponding author. Djahida Sidane *(D. Sidane)*
E-mail : djahida.sidane@univ-bejaia.dz

parameters on the bioactivity of the calcium phosphate ceramic powders synthesized in this study, the duration of the material's immersion in the SBF was fixed at 7 days.

2 Material and Methods

2.1 CaP based ceramic powder

Phosphorus pentoxide (Sigma Aldrich 97%) and calcium nitrate tetrahydrate (Sigma Aldrich 99%) were dissolved in absolute ethanol to form two solutions with concentrations of 0.5 M and 1.67 M, respectively. These solutions were mixed to obtain hydroxyapatite sol with a Ca/P molar ratio of 1.67 and continuously stirred for 24 hours and then closely capped and aged to complete the sol-gel transition process. The resultant colloidal solution was dried in an oven at 80°C for 24 hours. Finally, the dried gel was divided into four portions, and each portion was subjected to a specific temperature and/or duration as follows: 500°C for one hour, 600°C for one hour, 600°C for six hours, and 900°Cfor three hours, at a heating rate of 2 °C/min.

2.2 In vitro test

The bioactivity of the synthesized powders was tested in the SBF solution previously prepared using Kokubo and Takadama's formulation [11]. The principle of the test is to make pellets from the synthesized powders and expose them to the physiological solution for a sufficient period of time. To form a pellet, 0.3 g of each powder was placed in a 14-mm-diameter mold and then compacted under vacuum for 2 to 4 minutes at a force of 7 kN using a laboratory hydraulic press (Thermo Fisher). The pellets were then immersed in the SBF solution with a surface area-to- volume ratio of 0.1 cm^{-1} and then placed in a Thermo Scientific™ MaxQ 4000 incubator under agitation (60 rpm) at 37 °C for 7 days. The SBF media were replaced with fresh solution each time a sample was taken to ensure that the solution remained physiologically relevant and maintained a consistent chemical composition. Once removed, the pellets were immediately rinsed with distilled water and then delicately dried [12].

2.3 Characterization of the pellets and SBF media

The microstructure of the pellets was investigated by infrared spectroscopy using "Perkin-Elmer Spectrum Two" Attenuated Total Reflection (ATR) spectrometer. The analysis was performed by pressing the pellet against the ATR crystal. The crystalline phase of the pellet was analyzed by X-ray diffraction (XRD) using "PANalytical X'Pert Pro MPD" diffractometer with radiation source (Cu-Kα = 1.5406 Å).

In addition, the average crystallite size (L) was calculated using the Debye-Scherrer equation:

$$L_{hkl} = \frac{K\lambda}{\beta \cos\theta} \quad (1)$$

- λ is the wavelength of Cu-Kα radiation.
- β is the full width at middle height (the maximum intensity of the Bragg peak).
- θ is the diffraction angle.
- K is the Scherrer constant.

The morphological and elemental composition of the pellets was also analyzed after 7 days of incubation in the SBF solution. The pellet surfaces were examined using a "Hitachi TM3000" electron microscope and their chemical composition was determined using a "SciAps X-200" X-ray fluorescence (XRF) analyzer. As for the SBF media, they were analyzed after filtration using a "Thermo Scientific iCE 3000" series atomic absorption spectrometer equipped with an air-acetylene flame and a hollow-cathode calcium lamp. The pH of each sample was also measured using a "JENWAY 3510" pH meter. Measurements were performed three times. The values are presented as the mean and the corresponding standard deviation.

3 Results and Discussion

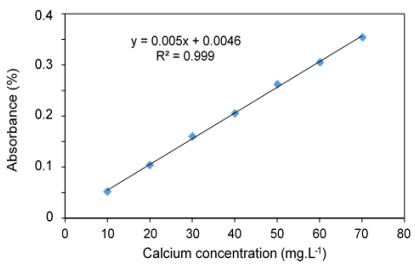

Fig.1. Atomic absorption analysis. Calibration curve.

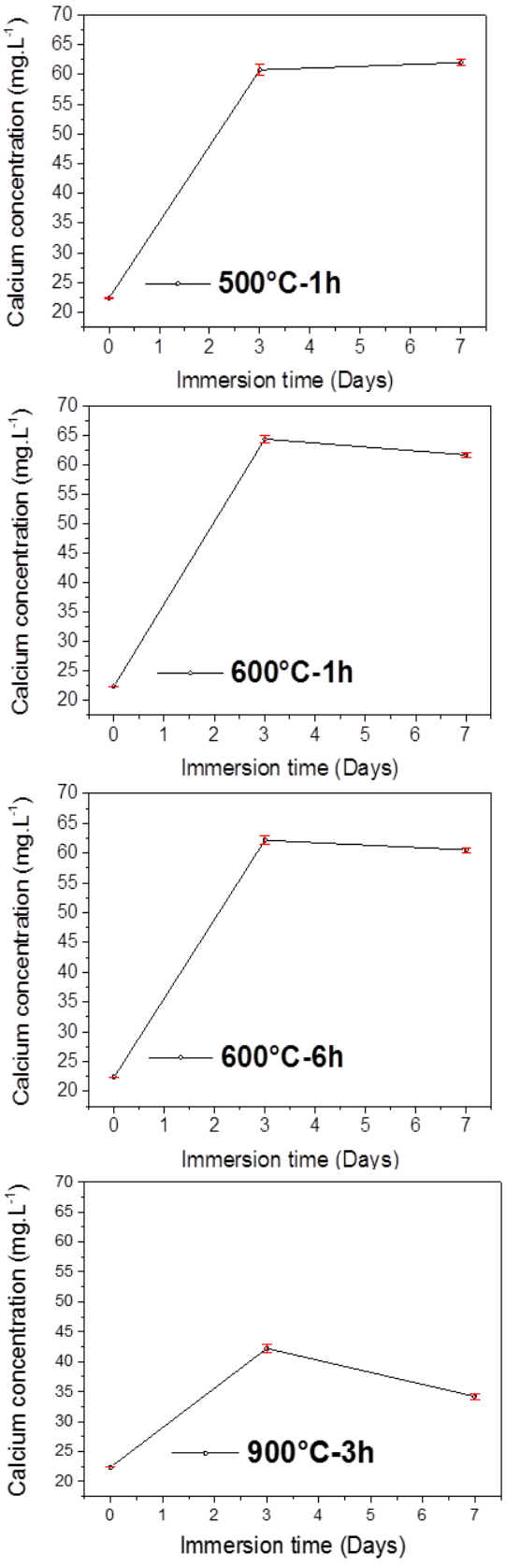

Fig.2. Variation in calcium concentration in the SBF medium as a function of the immersion time of the HAP pellets.

The calcium concentrations of the SBF media collected after soaking the pellets (500°C-1h, 600°C-1h, 600°C-6h and 900°C-3h) for 3 days and 7 days were determined by measuring the absorbance of standard samples of known concentrations (Figure 1).

The initial concentration of the SBF medium before immersion of the pellets was around 22.4 mg/L (Figure 2). For all samples, the Ca concentration increased with immersion time and reached after 3 days maximum values of 60.78 ± 0.96 mg/L for HAP calcined at 500°C, 62.17 ± 0.73 mg/L for HAP calcined at 600°C for 1 hour, 64.37 ± 0.64 mg/L for HAP calcined at 600°C for 6 hours, and 42.2 ± 0.70 mg/L for HAP calcined at 900°C. After 7 days of immersion, the Ca concentration in the SBF in contact with HAP

calcined at 500°C continued to increase, reaching a value of 62 ± 0.52 mg/L. While for HAP calcined at 600°C, the calcium concentration decreased to an average value of 61 mg/L and reached 34.2 ± 0.48 mg/L for HAP calcined at 900°C. The increase in calcium ion concentration in the SBF medium is due to the dissolution of HAP, while its decrease is attributed to the migration of Ca^{2+} ions from the SBF solution to the surface of HAP, as can be seen in the case of the samples calcined at 600°C and 900°C. This process is known as precipitation. It has been reported that after immersion and dissolution, HAP exposes its hydroxyl and phosphate groups, resulting in a negative surface that attracts Ca^{2+} ions present in SBF to form an amorphous calcium-rich phosphocalcic layer, which then interacts with the phosphate ions present in the SBF to form a calcium-poor phosphocalcic layer. Finally, this layer crystallizes into bone-like apatite [15].

The pH values of the SBF solutions measured after 7 days of immersion are shown in Table 1.

Table 1. pH values of the SBF media.

Samples	pH	
	0 day	7 days
500°C-1h	7.440 ± 0.02	7.442 ± 0.02
600°C-1h		7.335 ± 0.01
600°C-6h		7.324 ± 0.02
900°C-3h		7.305 ± 0.03

Compared to the initial value, the pH of the SBF medium in contact with HAP calcined at 500 °C increased slightly due to the dissolution of the HAP [16]. In contrast, the pH of the SBF media corresponding to HAP calcined at 600°C and 900°C tends to decrease. This phenomenon can be explained by the consumption of OH^- ions from the SBF during the formation of the apatite layer on the surface of the HAP [17]. The pH measurement results are in accordance with those obtained by atomic absorption spectrometry.

Figures 3a-d show the infrared spectra of the pellets before and after 7 days of immersion in the SBF solution.

The infrared spectra recorded for all samples prior to immersion show peaks at 473 cm^{-1}, 563 cm^{-1}, 600 cm^{-1}, 964 cm^{-1}, 1025 cm^{-1}, and 1089 cm^{-1}, which are attributed to PO_4^{3-} ions. The shoulder peak appearing at 630 cm^{-1} corresponds to the OH^- stretching vibration modes. The bands observed at 873 cm^{-1} and in the 1400–1600 cm^{-1} range are attributed to CO_3^{2-} ions. These absorption bands characterize the structure of crystalline carbonated hydroxyapatite. The presence of carbonate groups results from a partial substitution of PO_4^{3-} ions by CO_3^{2-} ions [18].

It should be noted that the vibrational peaks located around 3570 cm^{-1}, corresponding to the OH^- vibrations in the HAP lattice, are not clearly visible due to the limitations of the ATR spectroscopy technique in this region. After immersion, the intensity of the peaks of HAP calcined at 600°C for 6 hours decreased significantly. This can be explained by a marked dissolution process–the maximum calcium concentration in the SBF medium recorded for this sample was 64.37 mg/L or, more likely, by a loss of mass. In contrast, the infrared spectrum of the sample calcined at 900°C shows an increase in peak intensity, indicating that the precipitation process is predominant–the minimum calcium concentration in the SBF medium recorded for this sample was 34.2 mg/L. This contributed to a change in the microstructure of the powder calcined under these conditions. In fact, the OH^- band located at 630 cm^{-1} was no longer detected. Regarding the disappearance or reduction in the intensity of the OH functional group bands in the infrared spectrum obtained for the sample calcined at 900°C for 3 hours after immersion, we believe this is related to the depth resolution of the ATR technique and the newly precipitated bone-like apatite layer. Indeed, since the intensity of the structural OH groups of HAP, located at 630 cm^{-1}, is low, their signal was significantly attenuated due to the formation of bone-like apatite covering the sample's surface which made it difficult to detect the OH groups using ATR. For the samples calcined at 500°C and 600°C for 1 hour, the absorption bands did not undergo any significant changes.

The diffraction patterns of the samples before and after immersion in the SBF solution are presented in Figure 4 and Figure 5, respectively. Accordingly, to International Center for Diffraction Data (ICDD) patterns, the diffraction diagrams show peaks corresponding to the HAP structure, (JCPDS 9-0432) as the major crystalline phase. The characteristic triple peaks of HAP were observed at (211), (112), and (300) for 2θ values ranging between 31° and 33°. As shown in Figure 4, the intensity and sharpness of the HAP peaks became more pronounced as the calcination temperature increased from 500°C to 900°C. It is well known that the intensity of the peaks provides an indication of the degree of crystallinity of the samples [19].

Moreover, XRD patterns of HAP powders calcined at 600°C for 1 hour and 900°C for 3 hours, show minor secondary phases of β-tricalcium phosphate (β-$Ca_3(PO_4)_2$, JCPDS 9-169), and calcium oxide (CaO, JCPDS 37-1497) resulting from the thermal decomposition of hydroxyapatite. But, at 600°C, once the calcination time is increased from 1 hour to 6 hours, the peaks corresponding to β-TCP and CaO were no longer visible.

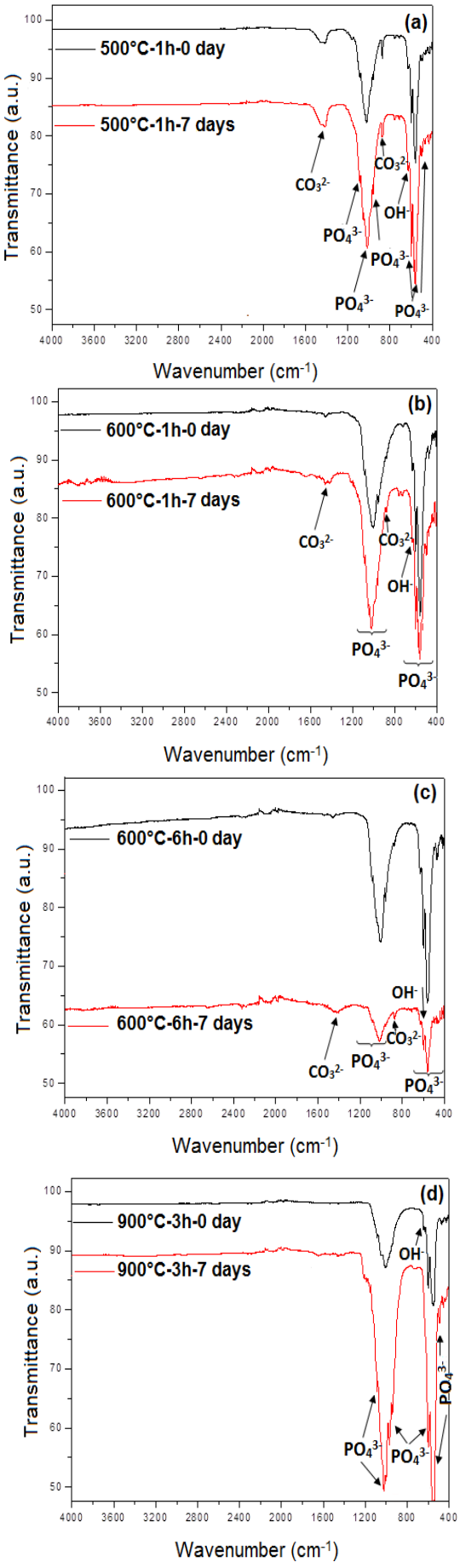

Fig.3. Infrared spectra of the pellets before and after immersion in SBF solution for 7 days.

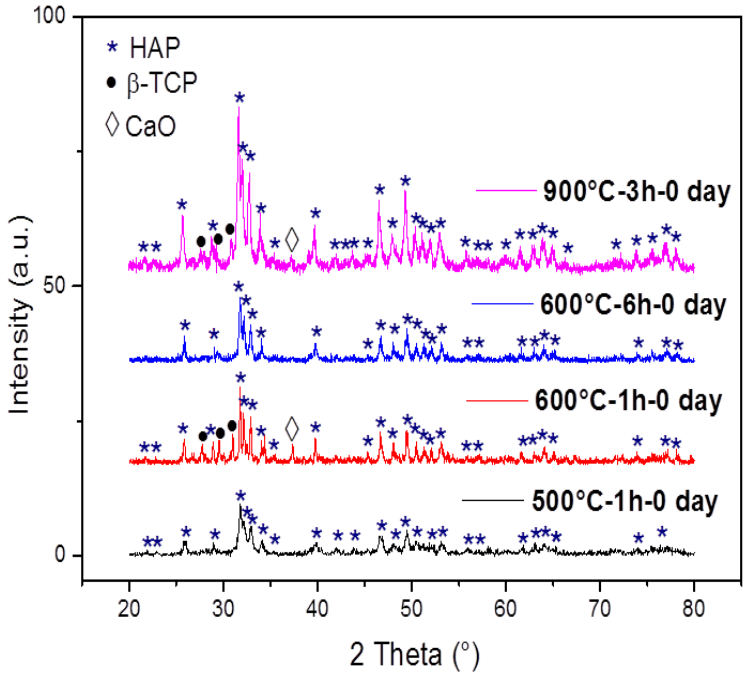

Fig.4. X-ray diffraction patterns of pellets before immersion in SBF solution.

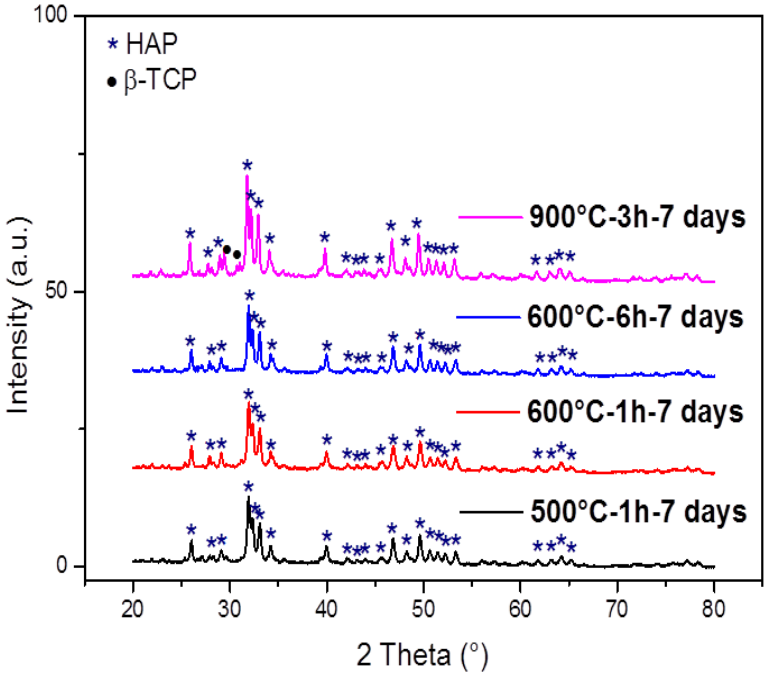

Fig.5. X-ray diffraction patterns of pellets after immersion in SBF solution for 7 days.

Thus, variations in temperature and calcination time have an impact not only on the crystallinity but also on the purity of the HAP powder [20]. Figure 5 shows the characteristic diffraction peaks of hydroxyapatite for all samples but their resolution decreased compared to the non-immersed samples.

In addition to HAP phase, the diffraction pattern of sample calcined at 900 ℃ for 3 hours shows main peaks corresponding to tricalcium phosphate, indicating that the β-TCP phase which is known to be a bioactive and highly resorbable ceramic [6] is still present in this powder. Whereas no diffraction peaks for calcium oxide were detected in any of the samples likely because this phase is present in very small quantities in the powders, so that the corresponding main peak located at 37.34° is no longer visible. It should be noted that the presence of the calcium oxide phase increases the calcium/phosphorus ratio in tricalcium phosphate, which plays an important role in the degradation rate of calcium phosphate-based ceramics [21]. The broadening of the diffraction peaks, as in the case of HAP calcined at 500°C (before and after immersion) and at 600°C (after immersion) indicates a decrease in the size of the crystallites. In fact, sharper and narrower peaks generally, associated with a higher overall degree of crystallinity indicate larger crystallite sizes [22]. The average crystallite sizes of the powders, are presented in Table 2.

Table 2. Crystallite sizes of HAP pellets before and after immersion in SBF solution.

Samples	Crystallite size L (nm)	
	Before immersion	After immersion
500°C-1h	34.9576	32.2902
600°C-1h	43.0153	35.8668
600°C-6h	42.7882	41.1203
900°C-3h	49.3323	46.1032

By increasing the calcination temperature from 500°C to 900°C, the values of the crystallite size increased too. Nevertheless, it was observed that extending the calcination time had no significant effect on the crystallite size of the powders calcined at 600°C. Whereas, the immersion of the powders in SBF solution resulted in a decrease of the crystallite size mainly for HAP calcined at 600°C for 1 hour. Predoi et al. [23] demonstrated

that immersion in SBF had a significant effect on HAP powder, resulting in a reduction in crystallite size. We can also note that the two powders calcined at 600°C for 6 hours and 900°C for 3 hours have almost the same crystallite sizes.

The CaO and β-TCP phases were identified in samples calcined at 600°C for 1 hour and at 900°C for 3 hours. It has been reported that CaO can be obtained through the complete decomposition of calcium carbonate depending on the processing atmosphere [24], but no crystalline $CaCO_3$ phase was detected by X-ray diffraction. This suggests that the formation of CaO results from the decomposition of the HAP bioceramic [25]. In turn, the formation of tricalcium phosphates could be associated with a reaction of CaO with phosphate ions released from the HAP lattice due to the incorporation of CO_3^{2-} [26] as confirmed by the infrared analysis. After immersion, both the CaO and β-TCP phases completely disappeared from the powder that had been calcined at 600°C for one hour, as CaO reacts completely with water to release calcium ions; whereas β-TCP, which is highly soluble, releases both Ca^{2+} ions and phosphate ions (PO_4^{3-}) into the solution. In the case of the powder pellet calcined at 900°C, the β-TCP partially dissolved, most likely due to the degree of crystallization of this powder or the amount of β-TCP present in this powder compared to the powder calcined at 600°C-1h.

Significant microstructural changes are observed particularly for HAP calcined at 900°C, due to the disappearance of the peak located at 630 cm^{-1}, corresponding to the hydroxyl groups that characterize the hydroxyapatite structure. However, the results of X-ray diffraction analysis indicate a main crystalline phase of hydroxyapatite and, in minor quantity, the presence of β-tricalcium phosphate. Therefore, the absence of the characteristic infrared peak of OH groups could be explained by the fact that the pellet surface was covered with a layer of amorphous calcium phosphate when it was immersed in the SBF solution, which masked or attenuated the bending vibration of the OH groups. It is known that the infrared spectrum of amorphous calcium phosphate presents several bands in the different vibrational regions of the PO_4 groups, but these bands are often difficult to distinguish due to band overlap and broadening [27]. We can therefore assume that this is due to the precipitation of a thin, and non-uniform layer of calcium phosphate, which partially covered the surface of the HAP pellet and was too amorphous to be detected by XRD analysis. The β-TCP phase, for its part, may promote the deposition of an apatite layer on its surface [14].

Figure 6 shows the Ca and P elemental composition of the pellets before and after 7 days of immersion in the SBF solution.

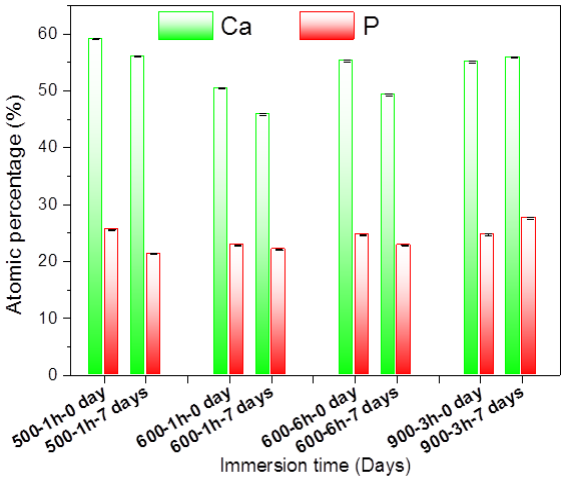

Fig.6. X-ray fluorescence analysis of the pellets.

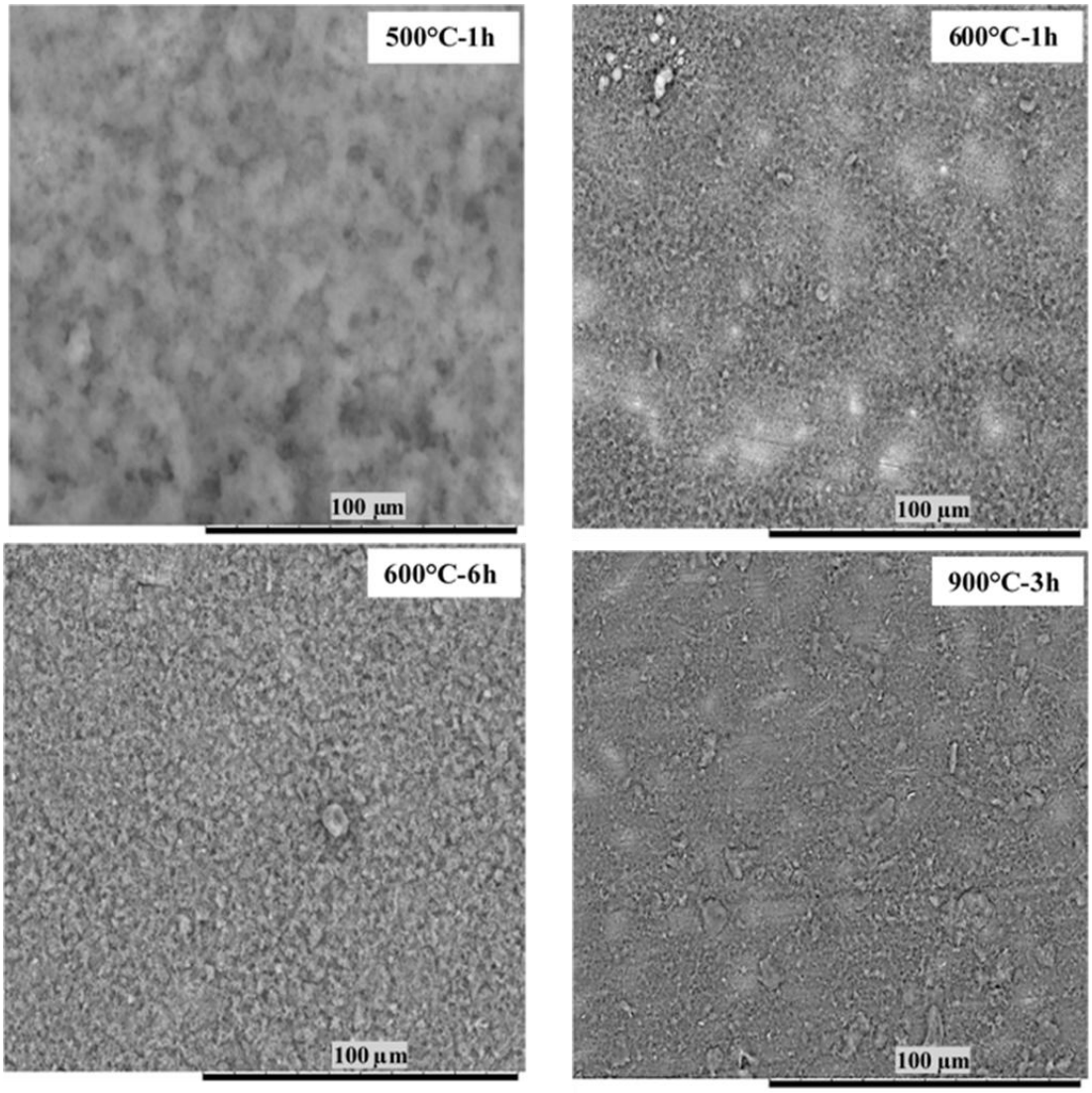

Fig.7. Microscopy images of pellets immersed for 7 days.

The increase in the atomic percentage of Ca (from 55.06 ± 0.156% to 55.85 ± 0.148%) and P (from 24.64 ± 0.155% to 27.59 ± 0.158%) for the HAP pellet calcined at 900°C indicates the possibility of formation of a phosphocalcic layer on its surface.

The surface morphology of the pellets after 7 days of immersion in the SBF solution is shown in Figure 7. The sample calcined at 500°C (Fig. 7a) exhibits an amorphous and porous structure. At 600°C, by increasing the calcination time from 1 hour (Fig. 7b) to 6 hours (Fig. 7c), the surface of the samples became denser. The microscopic image of the surface of the HAP pellet calcined at 900°C (Fig. 7d) clearly shows the deposition of dispersed and agglomerated particles of various sizes, confirming the possibility of the formation of a non-uniform layer of calcium phosphate (CaP), as indicated by XRD, ATR, and XRF analyses. According to De Micco et al. [9], crystalline ceramics often give rise to HAP layers with a less uniform structure. Furthermore, it has been reported that the immersion of synthetic hydroxyapatite in SBF solution leads to the deposition of carbonated apatite on its surface, depending on several factors, including the surface structure [15, 28].

Furthermore, X-ray diffraction analysis showed that HAP calcined at 900°C exhibited a higher degree of crystallinity, which is consistent with the observations made using a scanning electron microscope. This clearly indicates that the 900°C pellet has the appropriate characteristics in terms of crystallite size and degree of crystallinity to induce the formation of biological apatite on its surface, even though, previous studies have shown that high temperatures reduce the bioactive properties of the HAP sintered up to 1200°C [15, 29]. Shi et al. [30] studied the factors dominating the in vitro bioactivity of HAP powder, including surface area, degree of crystallinity, and temperature. The authors reported that the bioactivity decreased as crystallinity increased, which is likely related to the increased driving force for hydroxycarbonate apatite phase formation; furthermore, the reaction rate is proportional to the surface area. The proposed underlying mechanism is that the surface of highly crystalline hydroxyapatite requires a high driving force for the formation of the hydroxycarbonate apatite phase. In addition, the smaller crystals would have higher surface energies compared to the large ones. Nucleation on these high-energy surfaces generally requires a smaller driving force than that for the induction of nucleation on a low-energy surface such as a well-crystallized surface [30]. Moreover, it has been reported that the process of apatite formation was shown sluggish on the HAP powder sintered at higher temperature because of the lower negative surface charge of the HAP sintered at higher temperature [15].

Thus, by optimizing the calcination parameters, it is possible to modify the physicochemical properties of synthetic hydroxyapatite-based ceramics in such a way as to promote the formation of a layer of biological apatite on their surface in contact with the physiological environment. This opens up new possibilities for the design of bioceramics with tailored properties for bone regeneration and replacement [29].

4 Conclusion

Combined analyses of HAP pellets before and after a 7-day immersion in the SBF solution confirmed the formation of a CaP phosphocalcic layer on the surface of hydroxyapatite calcined at 900°C. Given the duration of immersion, it can be inferred that the formation of the calcium phosphate layer depends on the surface structure of the material in contact with the SBF medium. Consequently, hydroxyapatite powder calcined at 900°C for 3 hours is considered to be a bioactive ceramic powder. This bioceramic powder has the ability to form an apatite layer on its surface, which promotes cell adhesion and proliferation and supports tissue regeneration.

Acknowledgements

The authors are grateful to the staff of the University Abderrahmane Mira of Bejaia, and particularly acknowledged Prof. Belkacem Benmerad from “Laboratoire de Physico-Chimie des Matériaux et Catalyse (LPCMC)” for the infrared analysis.

Declaration of Competing Interest

The authors declare that they have no known competing financial interests or personal relationships that could have appeared to influence the work reported in this paper.

References

[1] A. Magnaudeix, Calcium phosphate bioceramics: From cell behavior to chemical-physical properties, Frontiers in Biomaterials Science 1 (2022) 942104. https://doi.org/10.3389/fbiom.2022.942104
[2] S. Yala, M. Boustta, O. Gallet, M. Hindié, F. Carreiras, H. Benachour, D. Sidane, H. Khireddine, New synthesis method of HA/P(D,L)LA composites: Study of fibronectin adsorption and their effects in osteoblastic behavior for bone tissue engineering, Journal of Materials Science: Materials in Medicine 27 (2016) 140. https://doi.org/10.1007/s10856-016-5756-8
[3] D. Sidane, H. Khireddine, S. Yala, The hardness of the hydroxyapatite-titania bilayer coatings by microindentation and nanoindentation testing, Journal of Physics: Conference Series 939 (2017) 012027. https://doi.org/10.1088/1742-6596/939/1/012027
[4] D.F. Fitriyana, F.W. Nugraha, M.B. Laroybafih, R. Ismail, A.P. Bayuseno, R.C. Muhamadin, M.B. Ramadan, A.R.A. Qudus, J.P. Siregar, The effect of hydroxyapatite concentration on the mechanical properties and degradation rate of biocomposite for biomedical applications, IOP Conference Series: Earth and Environmental Science 969 (2022) 012045. https://doi.org/10.1088/1755-1315/969/1/012045
[5] X. Yuan, T. Wu, T. Lu, J. Ye, Comparison of physicochemical and biological properties of calcium phosphate cements incorporating different strontium-containing compounds, Ceramics International 51 (2025) 60094–60105. https://doi.org/10.1016/j.ceramint.2025.10.208
[6] M.G. Raucci, D. Giugliano, L. Ambrosio, Fundamental properties of bioceramics and biocomposites, in: I. Antoniac (Ed.), Handbook of Bioceramics and Biocomposites, Springer, Cham, 2015.
[7] S. Ferraris, S. Yamaguchi, N. Barbani, M. Cazzola, C. Cristallini, M. Miola, E. Vernè, S. Spriano, Bioactive materials: In vitro investigation of different mechanisms of hydroxyapatite precipitation, Acta Biomaterialia 102 (2020) 468–480. https://doi.org/10.1016/j.actbio.2019.11.024
[8] J. Wang, L. Zhang, K. Wang, Bioactive ceramic-based materials: Beneficial properties and potential applications in dental repair and regeneration, Regenerative Medicine 19 (2024) 257–278. https://doi.org/10.1080/17460751.2024.2343555
[9] S. De Micco, D. Bellucci, V. Cannillo, The assessment of bioactivity and biological responsiveness in bioactive glasses and ceramics: A review of available techniques, Materials 18 (2025) 4393. https://doi.org/10.3390/ma18184393
[10] P.A. Forero-Sossa, J.D. Salazar-Martínez, A.L. Giraldo-Betancur, B. Segura-Giraldo, E. Restrepo-Parra, Temperature effect in physicochemical and bioactive behavior of biogenic hydroxyapatite obtained from porcine bones, Scientific Reports 11 (2021) 11069. https://doi.org/10.1038/s41598-021-89776-2
[11] T. Kokubo, H. Takadama, How useful is SBF in predicting in vivo bone bioactivity? Biomaterials 27 (2006) 2907–2915. https://doi.org/10.1016/j.biomaterials.2006.01.017
[12] D. Sidane, H. Khireddine, Microstructural modification of calcium phosphate-based bioceramic materials by adding gelatin, Asia-Pacific Journal of Chemical Engineering 20 (2025) e70075. https://doi.org/10.1002/apj.70075
[13] T. Kokubo, Bioceramics and Their Clinical Applications, Woodhead Publishing Limited, UK, 2008.
[14] M. Furko, Bioglasses versus bioactive calcium phosphate derivatives as advanced ceramics in tissue engineering: Comparative and comprehensive study, current trends, and innovative solutions, Journal of Functional Biomaterials 16 (2025) 161. https://doi.org/10.3390/jfb16050161
[15] H.M. Kim, T. Himeno, T. Kokubo, T. Nakamura, Process and kinetics of bonelike apatite formation on sintered hydroxyapatite in a simulated body fluid, Biomaterials 26 (2005) 4366–4373. https://doi.org/10.1016/j.biomaterials.2004.11.022
[16] A. Singh, Hydroxyapatite, a biomaterial: Its chemical synthesis, characterization and study of biocompatibility prepared from shell of garden snail, Helix aspersa, Bulletin of Materials Science 35 (2012) 1031–1038. https://doi.org/10.1007/s12034-012-0384-5
[17] A. Alshemary, M. Akram, Y. Goh, U. Tariq, F. Butt, A. Abdolahi, R. Hussain, Synthesis, characterization, in vitro bioactivity and antimicrobial activity of magnesium and nickel doped silicate hydroxyapatite, Ceramics International 41 (2015) 11886–11898. https://doi.org/10.1016/j.ceramint.2015.06.003
[18] Z.H. Cheng, A. Yasukawa, K. Kandori, T. Ishikawa, FTIR study on incorporation of CO2 into calcium hydroxyapatite, Journal of the Chemical Society, Faraday Transactions 94 (1998) 1501–1505. https://doi.org/10.1039/A708581H
[19] D.G. Chukhchin, A.V. Malkov, I.V. Tyshkunova, L.V. Mayer, E.V. Novozhilov, Diffractometric method for determining the degree of crystallinity of materials, Crystallography Reports 61 (2016) 371–375. https://doi.org/10.1134/S1063774516030081
[20] S. Mondal, S. Park, J. Choi, T.T.H. Vu, V.H.M. Doan, T.T. Vo, B. Lee, J. Oh, Hydroxyapatite: A journey from biomaterials to advanced functional materials, Advances in Colloid and Interface Science 321 (2023) 103013. https://doi.org/10.1016/j.cis.2023.103013
[21] H. Wang, J.K. Lee, A. Moursi, J.J. Lannutti, Ca/P ratio on the degradation of hydroxyapatite in vitro, Journal of Biomedical Materials Research Part A 67 (2003) 599–608. https://doi.org/10.1002/jbm.a.10538
[22] A.D. French, M. Santiago Cintrón, Cellulose polymorphy, crystallite size, and the Segal crystallinity index, Cellulose 20 (2013) 583–588. https://doi.org/10.1007/s10570-012-9833-y
[23] D. Predoi, C.S. Ciobanu, S.L. Iconaru, K. Rokosz, S. Raaen, S.A. Predoi, S. Ţălu, M. Motelica-Heino, Comprehensive physicochemical and biological analysis of hydroxyapatite/dextran powders before and after

immersion in Kokubo solution, Langmuir 41 (2025) 17011–17034. https://doi.org/10.1021/acs.langmuir.5c01585
[24] I. Galan, F.P. Glasser, C. Andrade, Calcium carbonate decomposition, Journal of Thermal Analysis and Calorimetry 111 (2013) 1197–1202. https://doi.org/10.1007/s10973-012-2290-x
[25] A. Costescu, I. Pasuk, F. Ungureanu, A. Dinischiotu, M. Costache, F. Huneau, S. Galaup, P. Le Coustumer, D. Predoi, Physico-chemical properties of nano-sized hexagonal hydroxyapatite powder synthesized by sol-gel, Digest Journal of Nanomaterials and Biostructures 5 (2010) 989–1000.
[26] S.A. Siddiqi, U. Azhar, Carbonate substituted hydroxyapatite, in: A.S. Khan, A.A. Chaudhry (Eds.), Handbook of Ionic Substituted Hydroxyapatites, Woodhead Publishing Series in Biomaterials, 2020, pp. 149–173. https://doi.org/10.1016/B978-0-08-102834-6.00006-9
[27] C. Combes, C. Rey, Amorphous calcium phosphates: Synthesis, properties and uses in biomaterials, Acta Biomaterialia 6 (2010) 3362–3378. https://doi.org/10.1016/j.actbio.2010.02.017
[28] H.M. Kim, T. Himeno, M. Kawashita, T. Kokubo, T. Nakamura, The mechanism of biomineralization of bone-like apatite on synthetic hydroxyapatite: An in vitro assessment, Journal of the Royal Society Interface 1 (2004) 17–22. https://doi.org/10.1098/rsif.2004.0003
[29] A. Kurzyk, A. Szwed-Georgiou, J. Pagacz, et al., Calcination and ion substitution improve physicochemical and biological properties of nanohydroxyapatite for bone tissue engineering applications, Scientific Reports 13 (2023) 15384. https://doi.org/10.1038/s41598-023-42271-2
[30] D. Shi, G. Jiang, J. Bauer, The effect of structural characteristics on the in vitro bioactivity of hydroxyapatite, Journal of Biomedical Materials Research 63 (2002) 71–78. https://doi.org/10.1002/jbm.10087